Chemical Science

ROYAL SOCIETY OF CHEMISTRY

EDGE ARTICLE

View Article Online
View Journal | View Issue



Cite this: *Chem. Sci.*, 2025, **16**, 20275

All publication charges for this article have been paid for by the Royal Society of Chemistry

Received 30th June 2025
Accepted 29th August 2025

DOI: 10.1039/d5sc04819b

rsc.li/chemical-science

# Catalytic asymmetric isomerization/hydroboration of silyl enol ethers

Yisen Yao, Jintao Sun, Jie Li and Wanxiang Zhao *

Asymmetric remote hydroboration of olefins has emerged as an efficient strategy for the construction of chiral boronic esters. Conventional asymmetric alkene isomerizations rely on directing groups (OH, $NR_2$, carbonyl) for thermodynamic control *via* (hyper)conjugation, but their use restricts substrate scope and risks β-heteroatom elimination with transition-metal catalysts. We here reported a catalytic asymmetric isomerization/hydroboration of silyl enol ethers under mild conditions, enabling the efficient synthesis of enantioenriched boryl ethers. The chiral borylether products enable efficient access to valuable 1,*n*-diols and 1,*n*-amino alcohols, prevalent in bioactive molecules, and facilitate late-stage functionalization of complex architectures. Preliminary mechanistic studies reveal that this reaction involves a nondissociative chain-walking process and that the β-H elimination may contribute to the rate-limiting step.

## Introduction

Enantioselective transformation of alkenes plays an important role in asymmetric synthesis due to their ready availability, natural abundance, and frequent use as prochiral precursors.[1a] To date, transition-metal-catalyzed enantioselective functionalization of alkenes primarily occurs at the native positions of C=C bonds through migratory insertion, nucleophilic or electrophilic addition, encompassing well-established methods such as asymmetric hydrogenation,[1] hydrofunctionalization,[2] and difunctionalization[3] (Fig. 1a, mode I). The organometallic intermediates **I** generated in the transition-metal-catalyzed functionalization of olefins may alternatively go through β-hydride elimination and reinsertion, resulting in positional olefin isomerization and the formation of a chiral center at the native C=C bond position, namely asymmetric functionalization-isomerization shown in Fig. 1b (Fig. 1b, mode II). However, this mode usually requires functional groups such as OH, $NR_2$, Ar, or carbonyl groups to provide thermodynamic driving force through the formation of (hyper)conjugated isomers.[4] For instance, catalytic enantioselective isomerization of alkenes (Fig. 1b, R = H) is mainly limited to allylic amines, alcohols (or ethers), and homoallylic alcohols, as demonstrated by Noyori,[5] Fu,[6] Wendlandt,[7] Zhao,[8] and others.[9] Similarly, the enantioselective functionalization-isomerization (Fig. 1b, R ≠ H) is primarily restricted to alkenyl alcohols to provide carbonyl compounds with a remote newly formed stereocenter, as shown in the work of the Sigman group.[10] However, catalytic asymmetric isomerization functionalization of heteroatom substituted-alkenes is much less developed because the heteroatoms might go through β-heteroatom elimination rather than β-hydride elimination,[11] limiting their applications in organic synthesis. Therefore, the development of new strategies for enantioselective isomerization-functionalization of heteroatom-substituted alkenes is highly desirable.

The catalytic asymmetric isomerization of alkenes often necessitates a functional group as the driving force (Fig. 1b, mode II). However, endergonic isomerizations can also[4,12] be facilitated by an irreversible terminal-selective functionalization,[13] enabling remote C($sp^3$)–H bond functionalization[14] (Fig. 1c). This isomerization-remote functionalization process has shown significant progress in recent years as it offers rapid access to value-added functional molecules from readily available feedstocks.[4,15] Nonetheless, the enantioselective isomerization-remote functionalization of alkenes remains relatively underexplored and poses challenges in stereoselectivity and regioselectivity control, particularly for heteroatom-substituted alkenes[16] (Fig. 1c, mode III). Building on our previous work in organoboron chemistry,[17] including enantioselective native hydroboration[18] and remote C($sp^3$)–H borylation[14e] of silyl enol ethers, we report a catalytic and enantioselective remote borylation of silyl enol ethers derived from ketones. This strategy addresses thermodynamic challenges, β-oxygen elimination, and regio- and enantioselectivity control to yield enantioenriched borylethers with synthetic utility (Fig. 1d).

## Results and discussion

We initiated our investigation using silyl enol ether (*Z*)-**1a′** as the model substrate, $[Rh(cod)Cl]_2$ as the catalyst, LiOAc as the base, and HBpin as the hydroboration reagent. Initially,

*State Key Laboratory of Chemo and Biosensing, Advanced Catalytic Engineering Research Center of the Ministry of Education, College of Chemistry and Chemical Engineering, Hunan University, Changsha, China. E-mail: zhaowanxiang@hnu.edu.cn*

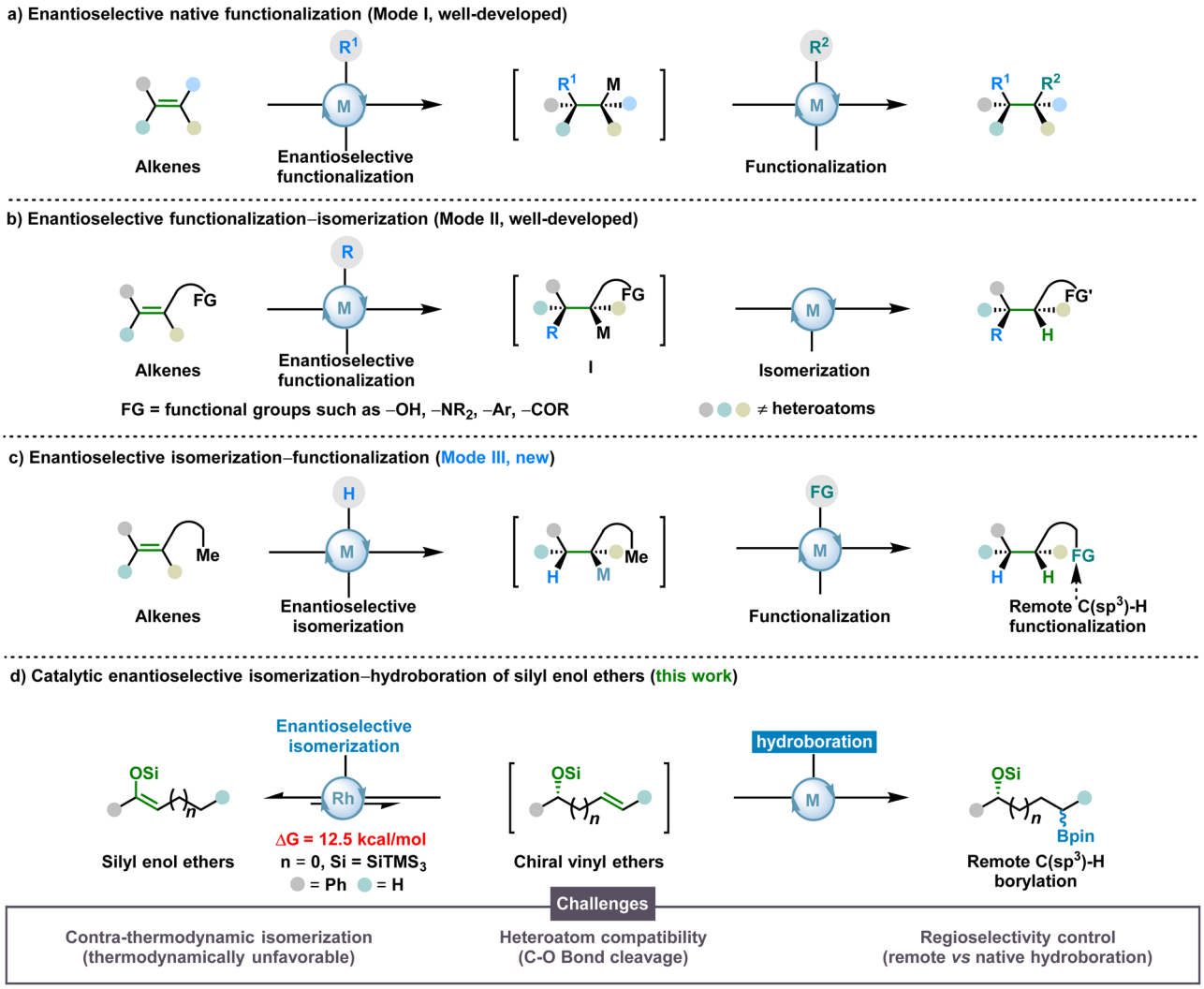


Fig. 1 (a) Enantioselective native functionalization of alkenes. (b) Enantioselective functionalization-isomerization of alkenes. (c) Enantioselective isomerization-functionalization of alkenes. (d) This work.

a variety of chiral ligands were examined. As shown in Fig. 2, entries 1–6, although no reaction was observed with ligands (*R*,*R*)-Sadphos (**L1**) and (*R*)-BINAP (**L2**), the desired product was obtained in 55% yield albeit with 55 : 45 er in the presence of (*R*,*R*)-BenzP* (**L3**). Based on these results, various sterically bulky and electron-rich chiral bidentate phosphine ligands, including (*R*,*R*)-QuinoxP* (**L4**), (*R*,*R*)-Ph-BPE (**L5**), and (*R*,*R*,*R*,*R*)-OMe-BIBOP (**L6**) were screened. The enantiomeric ratio was improved to 65 : 35 with (*R*,*R*)-QuinoxP*, while (*R*,*R*)-Ph-BPE (**L5**) gave the racemic product. Pleasingly, both the yield (90%) and the enantioselectivity (70 : 30 er) increased when (*R*,*R*,*R*,*R*)-OMe-BIBOP (**L6**) was employed. Encouraged by this delightful result, the analogue of BIBOP was studied.[19] As depicted, the substituents on the BIBOP have a great effect on the yields but only a subtle influence on enantioselectivity (**L7**–**L15**). Specifically, alkoxy groups on the BIBOP ligands are crucial for the reactivity of the Rh catalyst, as no product was obtained when R = H (**L7**). However, the enantiomeric ratio fluctuated around 65 : 35 regardless of the alkoxy substituents (**L8**–**L13**). Aromatic substituents were also used (**L14**, **L15**), but no improvement in results was achieved (see more details in the SI). We then turned our attention to investigating the reaction temperature (Fig. 2, entry 7). As expected, enantioselectivity increased as the reaction temperature decreased. Next, various silyl groups were also optimized. As shown, the er improved with increasing steric hindrance of the silyl group (Fig. 2, entries 7–11), and the super silyl ($SiTMS_3$) gave the highest er (88 : 12, Fig. 2, entry 11). The solvent effect was also surveyed. The use of DME and dioxane as solvents led to diminished yields, although no erosion in enantiopurity was observed (Fig. 2, entries 12–15). To our delight, a mixture solvent of THF/DCE (Fig. 2, entry 14) provided significantly better results both in yield (92%) and stereocontrol (92.5 : 7.5 er). In sharp contrast, no reaction was observed when DCE was used alone as the solvent (Fig. 2, entry 15). Enantioselectivity increased as the reaction temperature was lowered to 0 °C (Fig. 2, entry 16), and surprisingly, the enantiomeric ratio improved to 96 : 4 despite low conversion (48% yield). Finally, lowering the reaction temperature to 0 °C, increasing the

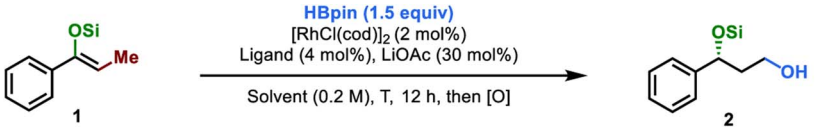


| Entry | Si | Ligand | Solvent | T (°C) | 2a (%)[a] | Er[b] |
|---|---|---|---|---|---|---|
| 1 | TES (**1a'**) | **L1** | THF | 70 | N.R. | - |
| 2 | TES (**1a'**) | **L2** | THF | 70 | N.R. | - |
| 3 | TES (**1a'**) | **L3** | THF | 70 | 55 | 55:45 |
| 4 | TES (**1a'**) | **L4** | THF | 70 | 46 | 65:35 |
| 5 | TES (**1a'**) | **L5** | THF | 70 | 45 | 50:50 |
| 6 | TES (**1a'**) | **L6** | THF | 70 | 92 | 70:30 |
| 7 | TES (**1a'**) | **L6** | THF | 30 | 88 | 81.5:18.5 |
| 8 | TMS (**1a''**) | **L6** | THF | 30 | 85 | 67:33 |
| 9 | TBS (**1a'''**) | **L6** | THF | 30 | 65 | 75:25 |
| 10 | TIPS (**1a''''**) | **L6** | THF | 30 | 82 | 81:19 |
| 11 | $SiTMS_3$ (**1a**) | **L6** | THF | 30 | 85 | 88:12 |
| 12 | $SiTMS_3$ (**1a**) | **L6** | DME | 30 | 56 | 88:12 |
| 13 | $SiTMS_3$ (**1a**) | **L6** | Dioxane | 30 | 68 | 87:13 |
| 14 | $SiTMS_3$ (**1a**) | **L6** | THF/DCE | 30 | 92 | 92.5:7.5 |
| 15 | $SiTMS_3$ (**1a**) | **L6** | DCE | 30 | N.R. | - |
| 16 | $SiTMS_3$ (**1a**) | **L6** | THF/DCE | 0 | 48 | 96:4 |
| **17[c]** | **$SiTMS_3$ (1a)** | **L6** | **THF/DCE** | **0** | **90** | **96:4** |
| **18[c,d]** | **$SiTMS_3$ (1a)** | **L6** | **THF/DCE** | **0** | **91** | **4:96** |

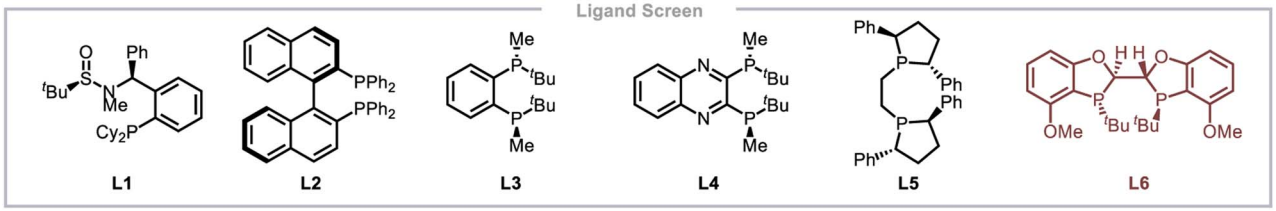


Fig. 2 Reaction condition optimization. General reaction conditions: **1** (0.1 mmol), HBpin (1.5 equiv.), $[RhCl(cod)]_2$ (2 mol%), ligand (4 mol%), LiOAc (30 mol%), solvent (0.5 mL), $T$ = 70 °C, 12 h. [a]Isolated yield. [b]Er were determined by HPLC on a chiral stationary phase. [c]$[RhCl(cod)]_2$ (5 mol%), ligand (10 mol%), 48 h. [d]Using (*S,S,S,S*)-**L6** as ligand. TIPS = triisopropylsilyl, TMS = trimethylsilyl, TBS = *tert*-butyldimethylsilyl, TES = triethylsilyl.

catalyst loading to 10 mol%, and prolonging the reaction time to 48 h gave the best result (90% isolated yield and 96 : 4 er, entry 17).

With the optimal reaction conditions in hand, we next explored the substrate scope of silyl enol ethers for this rhodium-catalyzed asymmetric remote hydroboration. As shown in Fig. 3, a diverse set of silyl enol ethers successfully participated in this enantioselective remote hydroboration, providing the corresponding 1,*n*-diol products in good yields and excellent enantioselectivities. The boronic esters were oxidized to the corresponding diols for ease of separation and determination of er. The mild reaction conditions were applicable to a broad range of linear alkyl silyl enol ethers with different chain lengths (**2a–2g**). It is worth mentioning that extra long-distant proceeded smoothly to furnish 1,12-diol **2e** in 89% yield and 94 : 6 er from phenyldodecanone-derived silyl enol ether under the standard reaction conditions. Importantly, an array of trisubstituted silyl enol ethers with different substituents at different positions on the phenyl ring underwent asymmetric isomerization/hydroboration to afford the valuable diol products in good efficiency. As described in Fig. 3, numerous substituents at *para*-position such as –Me (**2h**), –OMe (**2i**), and –Ph (**2j**) were well tolerated, leading to the corresponding diols in good yields and ers. Additionally, although the substrate **1k** with F at *ortho*-position gave a lower yield (46%) due to the low conversion, it exhibited a subtle influence on the enantioselectivity (89 : 11 er). Of particular note was that a broad range of functional groups including electron-donating groups and electron-withdrawing groups (**2l–2v**), such as –Ph, $–CH_2OBn$, –OMe, –F, –Cl, –Br, $–CF_3$, $–OCF_3$, and –TMS, were all compatible under the mild reaction conditions, providing the corresponding products in 92 : 8–98 : 2 ers. Gratifyingly, a range of functional groups that readily undergo downstream functionalizations such as –Bpin, –OH, –TMS, acetal, and Bn-protected alcohol could all be well accommodated to afford the desired products in moderate yields (50–65%) and good enantioselectivities (**2w–2ab**). Notably, a free phenolic group (**1x**) was compatible, and the corresponding product **2x** was provided in moderate yield and high enantioselectivity (50%, 95 : 5 er). In addition to the phenyl groups, other aromatic

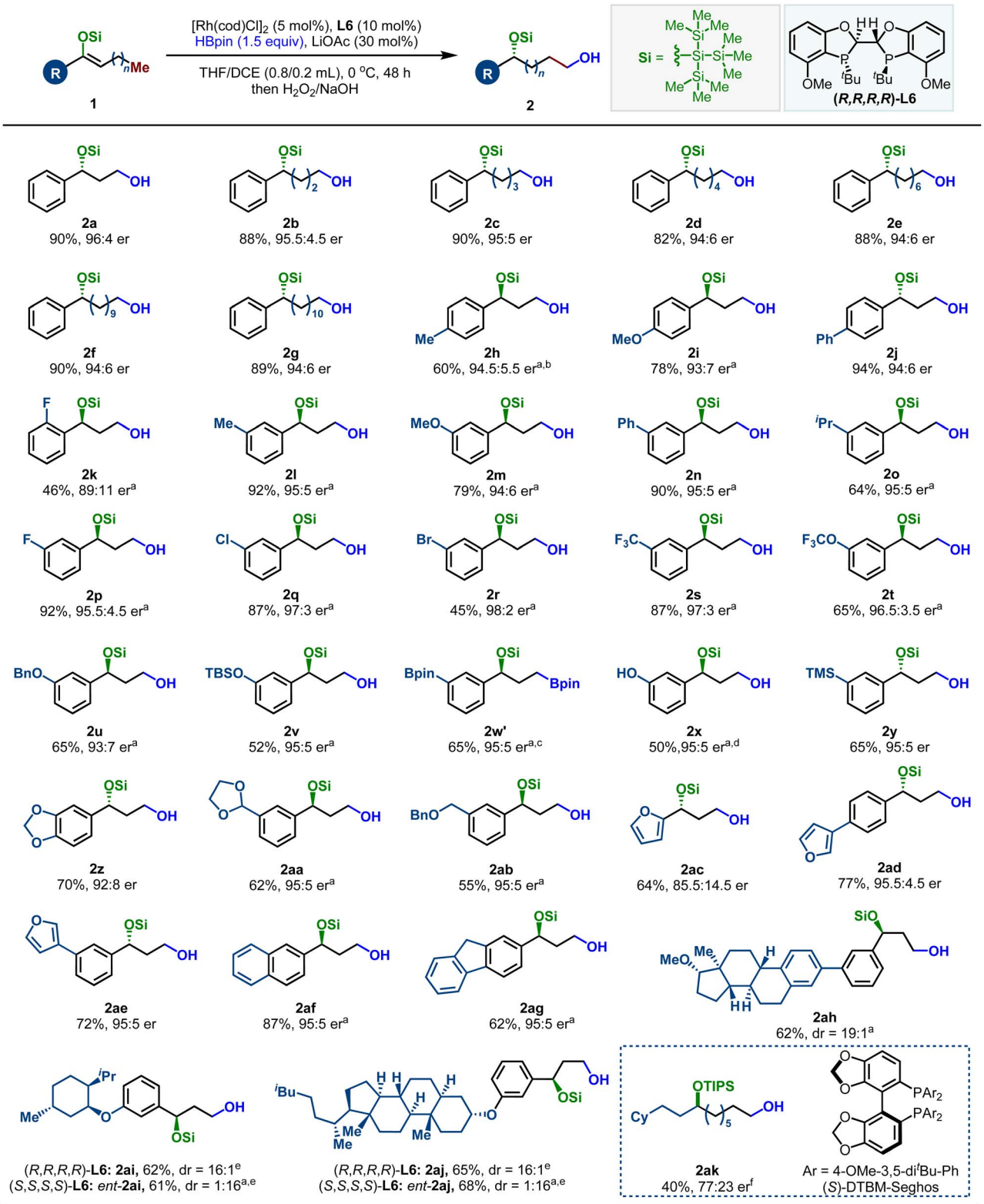


Fig. 3 Scope of Me-terminated silyl enol ethers. General reaction conditions: **1** (0.2 mmol), HBpin (1.5 equiv.), $[RhCl(cod)]_2$ (5 mol%), ligand (10 mol%), LiOAc (30 mol%), THF/DCE (0.8/0.2 mL), 0 °C, 48 h. Isolated yield. [a]Using (*S,S,S,S*)-**L6** as ligand. [b]Using hexane/2-methyl tetrahydrofuran/DCE (0.6/0.2/0.2 mL) as solvent. [c]Without oxidation. [d]The substrate is **1x** (see supporting information for details); HBpin (2.5 equiv.). [e]Dr was determined by HPLC. [f]**1ak** (0.2 mmol), HBpin (5.0 equiv.), $[RhCl(cod)]_2$ (5 mol%), (*S*)-DTBM-Segphos (10 mol%), LiOAc (2.0 equiv.), THF (1.0 mL), 110 °C, 48 h. Isolated yield.

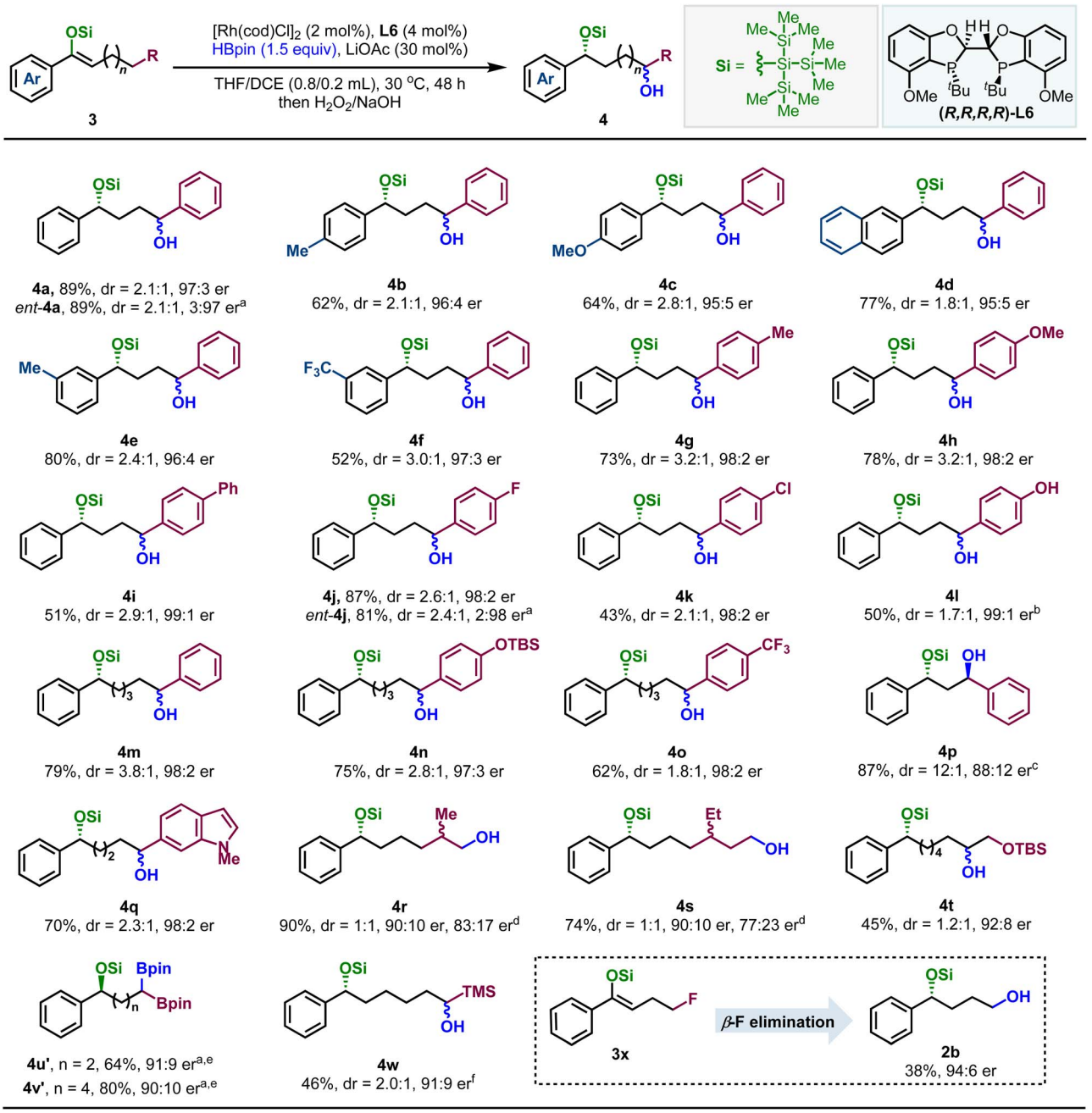


Fig. 4 Scope of R-terminated silyl enol ethers. Reactions conditions: **3** (0.2 mmol), HBpin (1.5 equiv.), $[Rh(cod)Cl]_2$ (2 mol%), ligand (4 mol%), LiOAc (30 mol%), THF/DCE (0.8/0.2 mL), 30 °C, 48 h. Dr was determined by analysis of $^1$H NMR spectra of unpurified mixtures. Er values of the major diastereoisomers are shown, and the er values of the minor diastereoisomers are shown in the SI. [a]Using (*S*,*S*,*S*,*S*)-**L6** as ligand. [b]The substrate is **3l** (see SI for details). [c]0 °C; [d]Dr was determined by analysis of HPLC spectra. [e]Without oxidation. [f]$^1$H NMR yield.

substituents such as naphthalene, fluorene, and furan could also be successfully incorporated into the products (**2ac–2ag**). To further demonstrate the applicability of this protocol, an array of silyl enol ethers derived from complex molecules were subjected to the established optimal conditions. We were pleased to find that the silyl enol ethers bearing dihydro cholesterol, estradiol, and (–)-menthol all underwent this enantioselective hydroboration to afford the diol products (**2ah–2aj**) in good yields and diastereoselectivities. The use of (*S*,*S*,*S*,*S*)-**L6** ligand gave the *ent*-**2ai** and *ent*-**2aj** good yields and diastereoselectivities. The reaction of dialkyl-substituted enol silyl ether **1ak** under standard conditions afforded racemic **2ak**. Pleasingly, the use of (*S*)-DTBM-Segphos instead of **L6** gave the desired product in 40% yield and moderate enantioselectivity (77 : 23 er).

Based on the success of enantioselective remote borylation of methyl-terminated silyl enol ethers, the generality of Rh-catalyzed asymmetric migratory borylation was further

evaluated by more challenging substrates, *i.e.*, non-methyl-terminated SEEs, which will be confronted with enantioselective, diastereoselective, and regioselective control issues. Pleasingly, as described in Fig. 4, we found that Ph-substrate **3a** reacted smoothly with HBpin to give the corresponding product **4a** in good yield (89%), high enantioselectivity (97 : 3 er), and reasonable diastereoselectivity under the optimized conditions. Moreover, an array of aryl-terminated substrates, with various substituents at different positions on the phenyl ring, underwent the desired asymmetric remote hydroboration, yielding valuable diol products with high efficiency. Various substituents at *para*- or *meta*-positions including electron-donating groups and electron-withdrawing groups (**4b–4l**), such as –Me, –OMe, $-CF_3$, –F, –Cl, –OTBS and –Bpin were all compatible under the mild reaction conditions, providing the corresponding products in 95 : 5 to 99 : 1 er. The moderate yield of *para*-phenyl-substituted substrate (51%) is due to the formation of hydrogenated products. Besides, the efficiency of

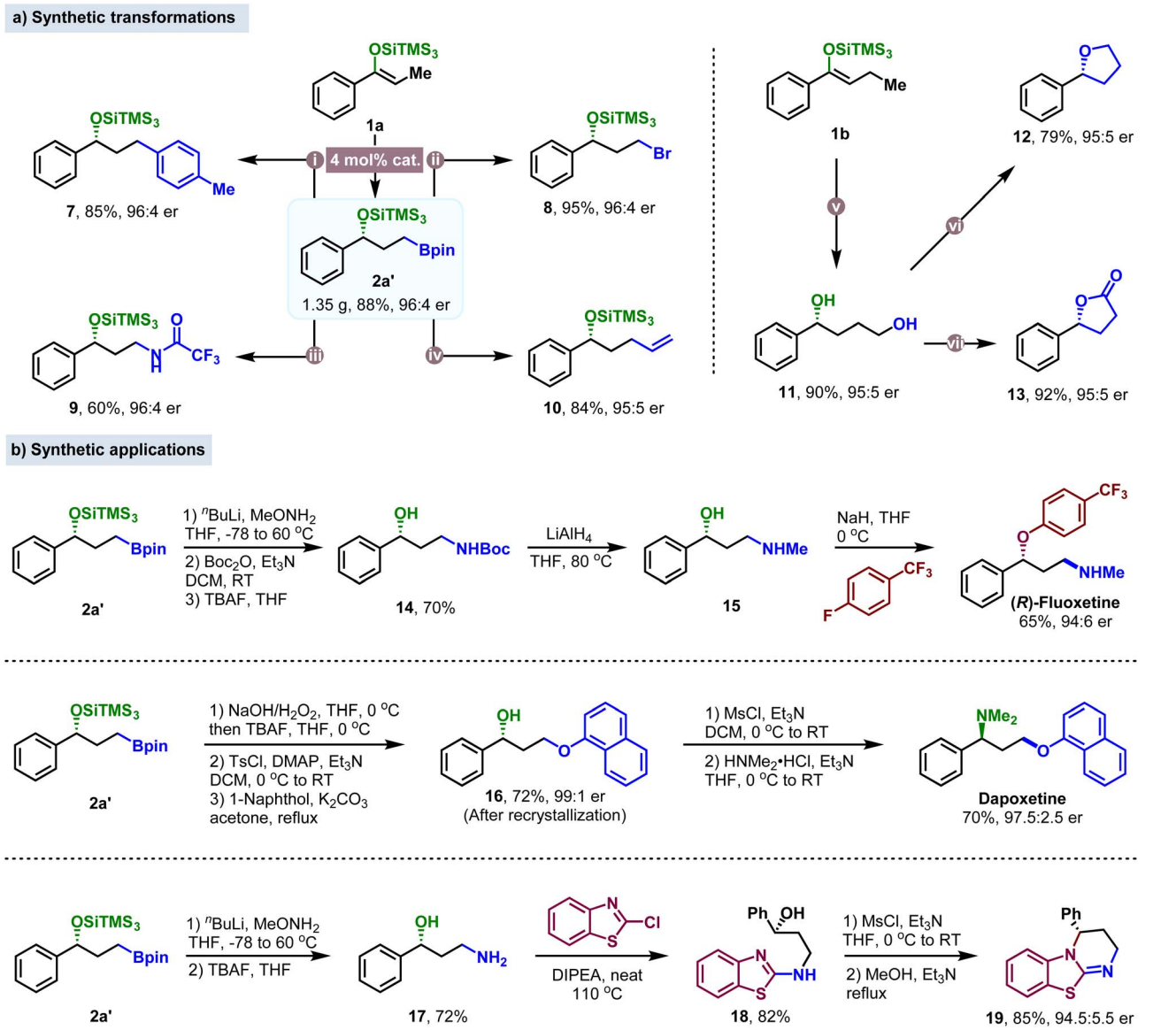


Fig. 5 (a) Synthetic transformations. Gram-scale reaction: **1a** (3.0 mmol), HBpin (1.5 equiv.), $[RhCl(cod)]_2$ (2 mol%), (*R*,*R*,*R*,*R*)-**L6** (4 mol%), LiOAc (30 mol%), THF/DCE (12.0/3.0 mL), 0 °C, 48 h. (i) $[Pd_2(dba)_3]$ (2 mol%), Ruphos (4 mol%), 4-bromotoluene (1.0 equiv.), $NaO^tBu$ (3.0 equiv.), toluene/$H_2O$, 80 °C, 24 h. (ii) 3,5-Bis(trifluoromethyl)bromobenzene (1.5 equiv.), $^n$BuLi (1.5 equiv.), NBS (1.5 equiv.), THF, −78 °C to RT. (iii) $KO^tBu$ (1.8 equiv.), $NH_2$-DABCO (1.2 equiv.), THF, 80 °C, 16 h, then TFAA (1.2 equiv.), 80 °C, 2 h. (iv) Vinylmagnesium bromide (4.0 equiv.), $I_2$ (4.0 equiv.), THF/MeOH, −78 °C to RT, 10 h. (v) **1b** (3.0 mmol), HBpin (1.5 equiv.), $[RhCl(cod)]_2$ (2 mol%), (*R*,*R*,*R*,*R*)-**L6** (4 mol%), LiOAc (30 mol%), THF/DCE (12.0/3.0 mL), 0 °C, 48 h; $NaOH/H_2O_2$ (1.5 equiv.), THF, 0 °C, 0.5 h; Then TBAF (1.5 equiv.), THF, 0 °C, 10 min. (vi) NaH (1.5 equiv.), $PO(OMe)_3$ (1.2 equiv.), CPME, RT, 12 h. (vii) $RuH_2(PPh_3)_4$ (10 mol%), (*E*)-4-phenylbut-3-en-2-one (2.0 equiv.), toluene, RT, 24 h. (b) Synthetic applications. See more details in the SI. Boc = *tert*-butoxycarbonyl, NBS = *N*-bromosuccinimide, TFAA = trifluoroacetic anhydride, TBAF = tetrabutylammonium fluoride, DABCO = triethylenediamine. DMAP = 4-dimethylaminopyridine, DIPEA = *N*,*N*-diisopropylethylamine, MsCl = methanesulfonylchloride.

migration is not affected by the alkyl chain length (**4m**–**4p**), and the corresponding products were provided with good yields and enantioselectivities. It's worth noting that **4p** could be obtained with good diastereoselectivity (12 : 1 dr). To our delight, the indole-terminated silyl enol ether (**3q**) can be converted to product **4q** successfully with good yield (70%) and excellent enantioselectivity (98 : 2 er). When isopropyl and 3-pentyl terminated silyl enol ethers (**3r**) and (**3s**) were treated with the optimized conditions, the isomerization was not affected, delivering the methyl borylation products efficiently. Silyl groups can also be used as terminating groups to furnish the corresponding diol (**3w**) in moderate yield and 91 : 9 er. Notably, we found that the boron was installed at the β position rather than the α position when the OTBS-terminated substrate (**3t**) was used, probably due to the steric hindrance. Besides, silyl enol ethers **3u** and **3v** with Bpin at the end of an alkyl chain, regardless of the chain length, were competent substrates, providing the *gem*-diboronate products with high efficiency. As expected, the fluorine (F) at the terminal position (**3x**) was incompatible, leading to the formation of the diol product **2b** in 38% yield (poor conversion) *via* defluorination.[20]

The alkyl boronates are versatile building protocol that might serve as a powerful platform to convert C($sp^3$)–H bonds into a variety of functional groups *via* the alkyl boronates generated in Fig. 5 by this asymmetric remote C($sp^3$)–H borylation. To demonstrate this point, a series of synthetic transformations of **2a′** were studied. First, a gram-reaction of substrate **1a** (3.0 mmol) was carried out, which proceeded smoothly to afford the desired alkyl boronate **2a′** in 88% yield and 96 : 4 er. Subsequently, Pd-catalyzed Suzuki–Miyaura[21] coupling of **2a′** with 4-bromotoluene was conducted, affording the product **7** in 85% yield and 96 : 4 er (Fig. 5a-i). The product **2a′** was then treated with the protocol developed by Aggarwal,[22] delivering the bromination product **8** in excellent yield (95%) and 96 : 4 er (Fig. 5a-ii). Furthermore, the amination reaction of boronate **2a′** *via* the protocol developed by Liu[23] was achieved in the presence of $NH_2$–DABCO and KO$^t$Bu, and the subsequent protection with TFAA gave the synthetically valuable amnio alcohol product **9** in 60% yield and 96 : 4 er (Fig. 5a-iii). The treatment of **2a′** with vinyl magnesium bromide and $I_2$ successfully furnished the desired product **10** in 84% yield and 95 : 5 er (Fig. 5a-iv), which could undergo further C=C bond functionalization to give a more complex fragment.[24] Considering that various types of 1,*n*-diols can be readily prepared *via* this enantioselective isomerization and hydroboration, and are widely applied in organic synthesis, the use of 1,4-diol **11** as a valuable building block for the synthesis of chiral **12** (ref. 25) and lactone **13** (ref. 26) was also demonstrated, suggesting this method may find broad applications in the synthesis of pharmaceutical and bioactive molecules, given the ubiquity of tetrahydrofuran and lactone skeletons.

The synthetic utilities of this approach were further demonstrated by the synthesis of chiral pharmaceutical molecules and catalysts. Starting from chiral alkyl boronate **2a′**, (*R*)-fluoxetine, an antidepressant, was prepared in 65% yield and 94 : 6 er *via* the amination[27] with $MeONH_2$ and $^n$BuLi, the reduction with $LiAlH_4$, and the $S_NAr$ reaction with 4-fluorobenzotrifluoride (Fig. 5b). In addition, dapoxetine, which is used to treat male sexual dysfunction, was successfully synthesized with good yield and excellent enantioselectivity (97.5 : 2.5 er). The synthesis involved Ts-protection of 1,3-diol, an $S_NAr$ reaction with 1-naphthol, followed by protection and an $S_N2$ reaction with dimethylamine hydrochloride. It is worth noting that chiral amino alcohol **17**, as a versatile synthon, could be prepared in high efficiency *via* the asymmetric migratory hydroboration of silyl enol ether **1a** and could be used in the synthesis of organic catalyst **19** (ref. 28) through the amination of chlorobenzothiazole and the cyclization of intermediate **18**.

Control experiments for stereoselectivity were conducted to investigate the geometry effect of the carbon–carbon double bond (Fig. 6a). Substrate **1s** was used as a model substrate because *Z*-**1s** and *E*-**1s** can be separated by column chromatography. Under the standard conditions, *Z*-**1s** reacted smoothly with HBpin to give the product *ent*-**2s** in 87% yield and 97 : 3 er (Fig. 6a, eqn (1)). The use of *E*/*Z* mixture led to the isolation of *ent*-**2s** in 39% yield and 97 : 3 er, and 52% of **1s** recovered (*E*/*Z* = 16/1) (Fig. 6a, eqn (2)). Additionally, only a trace amount of *ent*-**2s** was observed when **1s** (*E*/*Z* = 16/1) was subjected to the standard reaction conditions (Fig. 6a, eqn (3)). These results suggest that the reaction proceeds stereospecifically, as the significant steric hindrance likely prevented the coordination of the Rh–H complex to alkenes or the subsequent migratory insertion step.

To confirm this viewpoint about the contra-thermodynamic isomerization, allylic silyl ether **I** was prepared and subjected to the standard reaction conditions. The reaction proceeded smoothly to afford racemic **2a′** in 72% yield without forming the isomerization product **1a** (Fig. 6a, eqn (4)), likely due to Rh–H migratory insertion into allylic silyl ether **I** favored **2a′** formation due to steric hindrance. To complement the experimental findings, density functional theory (DFT) calculations were then carried out. The enthalpy and Gibbs free energy of silyl enol ether **1a** and allylic silyl ether **I** were calculated. As shown in Fig. 1d, the silyl enol ether **1a** is more stable than the corresponding allylic silyl ether **I** by 12.5 kcal mol$^{-1}$, indicating that the isomerization from **1a** to **I** is a contra-thermodynamic process, and the irreversible terminal hydroboration provides the driving force for this contra-thermodynamic isomerization. To gain more insights into the reaction mechanism, we carried out a series of deuterium-labeling experiments. The reaction of **1a** with DBpin under the standard conditions proceeded smoothly to afford product *d*-**2a** in 94% yield, and deuterium incorporation was observed along the carbon chain (38%, 10%, 2%, 5% and 5%), respectively (Fig. 6b, eqn (1)). This result was consistent with the chain-walking mechanism. Likewise, the use of deuterated silyl enol ether **1a**-$d_1$ resulted in the formation of **2a**-$d_1$ in 92% yield with 10%, 4%, 50%, 12% and 12%, D atom incorporation at the shown positions (Fig. 6b, eqn (2)). The reaction of **1a**-$d_3$ with HBpin under the standard conditions afforded product **2a**-$d_3$ in 86% yield with 78%, 50%, 82% and 82% D atom incorporation at the α- and β-positions of a hydroxyl group (Fig. 6b, eqn (3)). The successful formation of *d*-**2b** from vinyl ether **1b′** with 10%, 10%, and 9% D atom

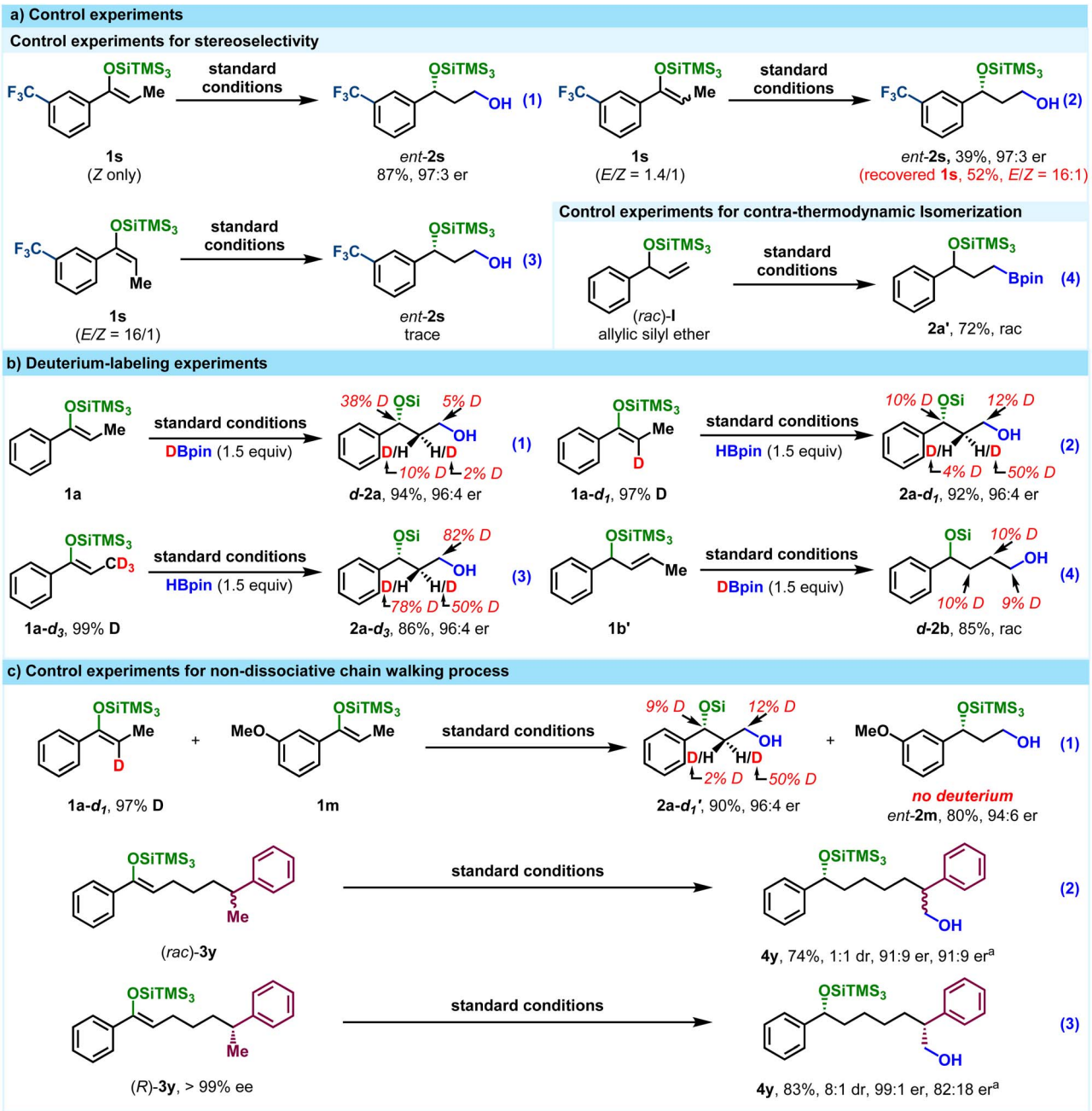


Fig. 6 (a) Control experiments. (b) Deuterium-labeling experiments. (c) Control experiments for non-dissociative chain walking process. [a]Dr was determined by analysis of HPLC spectra.

incorporation further verified the chain-walking process (Fig. 6b, eqn (4)). Based on these experimental results, we speculated that the migratory insertion of Rh–H into the silyl enol ether is not regioselective, but is irreversible, which might account for the D incorporation at the benzylic position in **2a**-$d_1$. Moreover, the chain walking process (iterative migratory insertion and β-H elimination) is reversible based on the deuterium labeling experiments. In addition, a cross-experiment between **1a**-$d_1$ and **1m** was conducted, providing product *ent*-**2m** in 80% yield without D incorporation (Fig. 6c, eqn (1)). Finally, control experiments using (*rac*)-**3y** and (*R*)-**3y** revealed distinct selectivity. (*rac*)-**3y** gave **4y** with 1 : 1 dr, 91 : 9 er and 91 : 9 er (Fig. 6c, eqn (2)), while (*R*)-**3y** afforded **4y** with 8 : 1 dr and er values of 99 : 1 and 82 : 18 (Fig. 6c, eqn (3)). These results indicated a non-dissociative chain-walking mechanism.[8]

To further shed light on the reaction mechanism, a set of kinetic experiments were carried out by using the initial rate method (Fig. 7a). As depicted, an inverse KIE of 0.98 was obtained when deuterated silyl enol ether **1a**-$d_1$ was subjected to the standard conditions (Fig. 7a-I and II), indicating that the migratory insertion of Rh–H into the silyl enol ether is less likely rate-limiting because hybridization change from $sp^2$ to $sp^3$ was

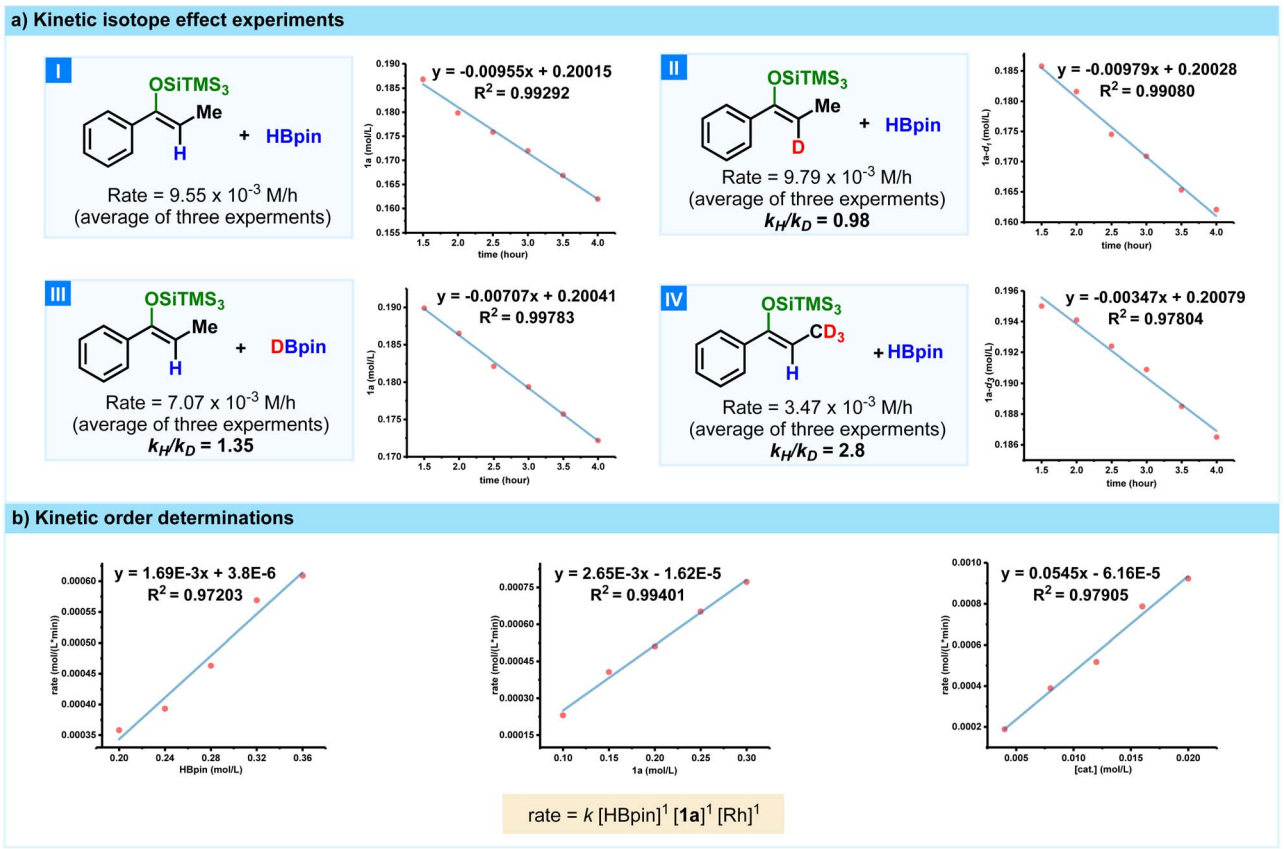


Fig. 7 (a) Kinetic isotope effect experiments. (b) Kinetic order determinations.

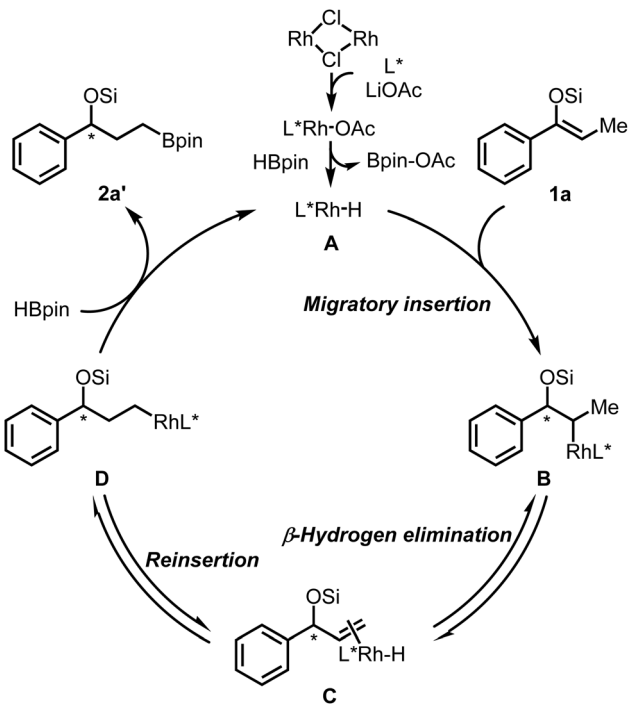


Fig. 8 Proposed mechanism cycle.

involved in this step. Moreover, the measurement of the reaction rates with HBpin and DBpin revealed a KIE of 1.35 (Fig. 7a-I and III), suggesting that the B–H bond cleavage is less likely to be rate-determining. Besides, the KIE experiment of deuterated silyl enol ether **1a**-$d_3$ with HBpin was explored, giving a KIE of 2.8 (Fig. 7a-I and IV) and indicating that β-hydride elimination may be the rate-limiting step.[29] Finally, kinetic experiments were carried out. We found that the reaction exhibited a first-order dependence on the catalyst, as well as on both **1a** and HBpin (Fig. 7b). These results suggested that β-hydride elimination likely contributed to the rate-limiting step.

Based on the experimental results, a plausible reaction mechanism is proposed, as illustrated in Fig. 8. The catalytic cycle initiates with the coordination of $[Rh(cod)Cl]_2$ with chiral ligand **L*** and LiOAc to form a rhodium complex. Subsequent reaction with HBpin yields the key Rh–H species **A**. Migratory insertion of Rh–H species **A** into the substrate **1a** generates intermediate **B**, which undergoes β-hydride elimination to afford the isomerized alkene complex **C**. Finally, reinsertion followed by metathesis with HBpin releases product **2a′** and regenerates the active Rh–H species **A**, thereby completing the catalytic cycle.

## Conclusions

In conclusion, we have developed a novel catalytic asymmetric isomerization/hydroboration of silyl enol ethers under mild reaction conditions, providing an efficient method for the construction of enantioenriched and synthetically-valued borylethers. This reaction showed a broad substrate scope of silyl

enol ethers and good functional group tolerance. Notably, various terminated groups, such as Me, Ar, protected alcohol, oxygen, boron, and silicon, were all compatible with delivering the value-added corresponding diols efficiently. This reaction overcomes the thermodynamically unfavorable isomerization, β-oxygen elimination, and the challenging regioselectivity and enantioselectivity control. Notably, the chiral borylether products can be converted to various value-added building blocks, such as halides, alkenes, 1,*n*-diol, lactones, and oxyheterocyclic rings. The practicability of this protocol in medicine and organic synthesis was also demonstrated by the successful synthesis of organic catalysts and drug molecules, including dapoxetine and fluoxetine. Preliminary mechanistic studies revealed that a nondissociative chain-walking process was involved, with the β-hydrogen elimination possibly contributing to the rate-limiting step. Further research on enantioselective contra-thermodynamic reactions and their applications is currently ongoing in our laboratory.

## Author contributions

W. Z. conceived the project and directed the work. W. Z., Y. Y. and J. L. wrote the paper. Y. Y. and J. S. prepared the supplementary information. Y. Y. and J. S. performed the experiments.

## Conflicts of interest

There are no conflicts to declare.

## Data availability

All data needed to evaluate the conclusions in the paper are present in the paper and/or the SI: synthetic details, characterization of products and substrates, and computational details. See DOI: **https://doi.org/10.1039/d5sc04819b**.

## Acknowledgements

We thank Y. X. (HNU) for the experimental assistance, C. L. (GZU) for assistance with the preparation of the manuscript and supporting information. We thank the National Natural Science Foundation of China (Grant No. 22271086, U24A20481 and 21971059), the National Program for Thousand Young Talents of China, the National Natural Science Foundation of China (32360689), the Science and Technology Project of Hunan Province (2024JJ3006) and the Hunan Provincial Innovation Foundation for Postgraduates (No. CX20230413).

## References

1 (*a*) C. Margarita and P. G. Andersson, *J. Am. Chem. Soc.*, 2017, **139**, 1346; (*b*) X. Cui and K. Burgess, *Chem. Rev.*, 2005, **105**, 3272; (*c*) S. Kraft, K. Ryan and R. B. Kargbo, *J. Am. Chem. Soc.*, 2017, **139**, 11630.

2 (*a*) J. Chen and Z. Lu, *Org. Chem. Front.*, 2018, **5**, 260; (*b*) F. Yuan, X. Qi, Y. Zhao, J. Jia, X. Yan, F. Hu and Y. Xia, *Angew. Chem., Int. Ed.*, 2024, **63**, e202401451; (*c*) B. Huang and Q. Li, *Chin. J. Org. Chem.*, 2024, **44**, 2611.

3 (*a*) R. I. McDonald, G. Liu and S. S. Stahl, *Chem. Rev.*, 2011, **111**, 2981; (*b*) J. R. Coombs and J. P. Morken, *Angew. Chem., Int. Ed.*, 2016, **55**, 2636; (*c*) C. Ji and D. Gao, *Chin. J. Org. Chem.*, 2024, **44**, 1385.

4 (*a*) E. Larionov, H. Li and C. Mazet, *Chem. Commun.*, 2014, **50**, 9816; (*b*) A. Vasseur, J. Bruffaerts and I. Marek, *Nat. Chem.*, 2016, **8**, 209; (*c*) H. Sommer, F. Julia-Hernandez, R. Martin and I. Marek, *ACS Cent. Sci.*, 2018, **4**, 153; (*d*) D. Fiorito, S. Scaringi and C. Mazet, *Chem. Soc. Rev.*, 2021, **50**, 1391.

5 (*a*) K. Tani, T. Yamagata, S. Otsuka, S. Akutagawa, H. Kumobayashi, T. Taketomi, H. Takaya, A. Miyashita and R. Noyori, *J. Chem. Soc., Chem. Commun.*, 1982, 600; (*b*) K. Tani, T. Yamagata, S. Akutagawa, H. Kumobayashi, T. Taketomi, H. Takaya, A. Miyashita, R. Noyori and S. Otsuka, *J. Am. Chem. Soc.*, 1984, **106**, 5208; (*c*) S. Inoue, H. Takaya, K. Tani, S. Otsuka, T. Sato and R. Noyori, *J. Am. Chem. Soc.*, 1990, **112**, 4897.

6 (*a*) K. Tanaka, S. Qiao, M. Tobisu, M. M. C. Lo and G. C. Fu, *J. Am. Chem. Soc.*, 2000, **122**, 9870; (*b*) K. Tanaka and G. C. Fu, *J. Org. Chem.*, 2001, **66**, 8177.

7 (*a*) G. Occhialini, V. Palani and A. E. Wendlandt, *J. Am. Chem. Soc.*, 2022, **144**, 145; (*b*) V. Palani and A. E. Wendlandt, *J. Am. Chem. Soc.*, 2023, **145**, 20053.

8 (*a*) T. L. Liu, T. W. Ng and Y. Zhao, *J. Am. Chem. Soc.*, 2017, **139**, 3643; (*b*) R. Z. Huang, K. K. Lau, Z. Li, T. L. Liu and Y. Zhao, *J. Am. Chem. Soc.*, 2018, **140**, 14647.

9 (*a*) Z. Wu, J. D. Laffoon, T. T. Nguyen, J. D. McAlpin and K. L. Hull, *Angew. Chem., Int. Ed.*, 2017, **56**, 1371; (*b*) R. Wu, M. G. Beauchamps, J. M. Laquidara and J. R. Sowa Jr, *Angew. Chem., Int. Ed.*, 2012, **51**, 2106; (*c*) V. Bizet, X. Pannecoucke, J. L. Renaud and D. Cahard, *Angew. Chem., Int. Ed.*, 2012, **51**, 6467; (*d*) L. Lin, K. Yamamoto, H. Mitsunuma, Y. Kanzaki, S. Matsunaga and M. Kanai, *J. Am. Chem. Soc.*, 2015, **137**, 15418–15421; (*e*) J. T. Han, J. Y. Lee and J. Yun, *Chem. Sci.*, 2020, **11**, 8961; (*f*) T. C. Jankins, R. Martin-Montero, P. Cooper, R. Martin and K. M. Engle, *J. Am. Chem. Soc.*, 2021, **143**, 14981; (*g*) K. Zhao and R. R. Knowles, *J. Am. Chem. Soc.*, 2022, **144**, 137.

10 (*a*) E. W. Werner, T. Mei, A. J. Burckle and M. S. Sigman, *Science*, 2012, **338**, 1458; (*b*) T. S. Mei, H. H. Patel and M. S. Sigman, *Nature*, 2014, **508**, 340; (*c*) H. H. Patel, M. B. Prater, S. O. Squire Jr and M. S. Sigman, *J. Am. Chem. Soc.*, 2018, **140**, 5895; (*d*) J. Liu, Q. Yuan, F. D. Toste and M. S. Sigman, *Nat. Chem.*, 2019, **11**, 710; (*e*) A. Bahamonde, B. Al Rifaie, V. Martin-Heras, J. R. Allen and M. S. Sigman, *J. Am. Chem. Soc.*, 2019, **141**, 8708.

11 (*a*) J. Cornella, C. Zarate and R. Martin, *Chem. Soc. Rev.*, 2014, **43**, 8081; (*b*) T. Iwasaki, Y. Miyata, R. Akimoto, Y. Fujii, H. Kuniyasu and N. Kambe, *J. Am. Chem. Soc.*, 2014, **136**, 9260; (*c*) S. Li, J. Li, T. Xia and W. Zhao, *Chin. J. Chem.*, 2019, **37**, 462; (*d*) C. Matt, A. Orthaber and J. Streuff, *Angew. Chem., Int. Ed.*, 2022, **61**, e202114044; (*e*) V. T. Tran, J. A. Gurak Jr, K. S. Yang and K. M. Engle, *Nat. Chem.*, 2018, **10**, 1126.

12 (*a*) J. V. Obligacion and P. J. Chirik, *J. Am. Chem. Soc.*, 2013, **135**, 19107; (*b*) X. Li, J. Jin, P. Chen and G. Liu, *Nat. Chem.*, 2022, **14**, 425; (*c*) Z. Wu, J. Meng, H. Liu, Y. Li, X. Zhang and W. Zhang, *Nat. Chem.*, 2023, **15**, 988; (*d*) N. G. Léonard, W. N. Palmer, M. R. Friedfeld, M. J. Bezdek and P. J. Chirik, *ACS Catal.*, 2019, **9**, 9034.

13 (*a*) W. Liu, Y. Zheng, Y. Mao, J. Chen, X. Ren, Z. Cheng and Z. Lu, *Org. Lett.*, 2022, **24**, 1158; (*b*) M. Hu and S. Ge, *Nat. Commun.*, 2020, **11**, 765; (*c*) C. Chen, H. Wang, T. Li, D. Lu, J. Li, X. Zhang, X. Hong and Z. Lu, *Angew. Chem., Int. Ed.*, 2022, **61**, e202205619; (*d*) J. Liu, J. Du, F. Yu, L. Gan, G. Liu and Z. Huang, *ACS Catal.*, 2023, **13**, 7995; (*e*) S. Hanna, B. Bloomer, N. R. Ciccia, T. W. Butcher, R. J. Conk and J. F. Hartwig, *Org. Lett.*, 2022, **24**, 1005.

14 (*a*) C. M. Macaulay, C. M. Macaulay, S. J. Gustafson, J. T. Fuller, D. Kwon, T. Ogawa, M. J. Ferguson, R. McDonald, M. D. Lumsden, S. M. Bischof, O. L. Sydora, D. H. Ess, M. Stradiotto and L. Turculet, *ACS Catal.*, 2018, **8**, 9907; (*b*) T. Ogawa, A. J. Ruddy and O. L. Sydora, *Organometallics*, 2017, **36**, 417; (*c*) A. J. Ruddy, O. L. Sydora, B. L. Small, M. Stradiotto and L. Turculet, *Chem.–Eur. J.*, 2014, **20**, 13918; (*d*) T. M. Saunders, S. B. Shepard, D. J. Hale, K. N. Robertson and L. Turculet, *Chem.–Eur. J.*, 2023, **29**, e202301946; (*e*) P. Zhao, J. Huang, J. Li, K. Zhang, W. Yang and W. Zhao, *Chem. Commun.*, 2022, **58**, 302.

15 (*a*) X. Chen, Z. Cheng, J. Guo and Z. Lu, *Nat. Commun.*, 2018, **9**, 3939; (*b*) C. Romano, D. Fiorito and C. Mazet, Remote Functionalization of α,β-Unsaturated Carbonyls by Multimetallic Sequential Catalysis, *J. Am. Chem. Soc.*, 2019, **141**, 1698; (*c*) F. Zhou, Y. Zhang, X. Xu and S. Zhu, *Angew. Chem., Int. Ed.*, 2019, **58**, 1754; (*d*) M. L. Scheuermann, E. J. Johnson and P. J. Chirik, *Org. Lett.*, 2015, **17**, 2716; (*e*) Y. Zhao and S. Ge, *Angew. Chem., Int. Ed.*, 2022, **61**, e202116133.

16 J. Li, S. Qu and W. Zhao, *Angew. Chem., Int. Ed.*, 2020, **59**, 2360.

17 (*a*) M. Zhang, Z. Liu and W. Zhao, *Angew. Chem., Int. Ed.*, 2023, **62**, e202215455; (*b*) M. Zhang, Z. Ye and W. Zhao, *Angew. Chem., Int. Ed.*, 2023, e202306248.

18 (*a*) W. Dong, X. Xu, H. Ma, Y. Lei, Z. Lin and W. Zhao, *J. Am. Chem. Soc.*, 2021, **143**, 10902; (*b*) W. Dong, Z. Ye and W. Zhao, *Angew. Chem., Int. Ed.*, 2022, **61**, e202117413.

19 G. Xu, C. H. Senanayake and W. Tang, *Acc. Chem. Res.*, 2019, **52**, 1101.

20 H. Amii and K. Uneyama, *Chem. Rev.*, 2009, **109**, 2119.

21 S. N. Mlynarski, C. H. Schuster and J. P. Morken, *Nature*, 2014, **505**, 386.

22 X. Liu, Q. Zhu, D. Chen, L. Wang, L. Jin and C. Liu, *Angew. Chem., Int. Ed.*, 2020, **59**, 2745.

23 R. Larouche-Gauthier, T. G. Elford and V. K. Aggarwal, *J. Am. Chem. Soc.*, 2011, **133**, 16794.

24 R. P. Sonawane, V. Jheengut, C. Rabalakos, R. Larouche-Gauthier, H. K. Scott and V. K. Aggarwal, *Angew. Chem., Int. Ed.*, 2011, **50**, 3760.

25 S. Asai, M. Kato, Y. Monguchi, H. Sajiki and Y. Sawama, *Chem. Commun.*, 2017, **53**, 4787.

26 Y. Ishii, K. Osakada, T. Ikariya, M. Saburi and S. Yoshikawa, *J. Org. Chem.*, 1986, **51**, 2034.

27 S. N. Mlynarski, A. S. Karns and J. P. Morken, *J. Am. Chem. Soc.*, 2012, **134**, 16449.

28 B. Viswambharan, T. Okimura, S. Suzuki and S. Okamoto, *J. Org. Chem.*, 2011, **76**, 6678.

29 M. Gomez-Gallego and M. A. Sierra, *Chem. Rev.*, 2011, **111**, 4857.